Simulation Studies on a Rotating Ring Disk Electrode System: Role of Supporting Electrolyte in Determination of Relevance of Ionic Migration

Sirshendu Guha
Process Design & Development Division, Engineers India Ltd, Kolkata, India

DOI 10.1002/aic.13903
Published online September 4, 2012 in Wiley Online Library (wileyonlinelibrary.com).

Most of the past theoretical works with the rotating ring disk electrode (RRDE) system have been restricted to situations where supporting electrolyte concentration is large enough so that the effects of migration of ionic species in the solution becomes negligible. In this work, effects of ionic migration have been investigated for a RRDE system by solving the differential equations describing mass transfer in presence of ionic migration using numerical technique. Two cases were considered for simulation, presence and absence of migration of ionic species. Results indicate that in presence of migration, collection efficiency of a RRDE system increases for all electrode geometries and concentration boundary layer thickness reduces. Results also indicate that collection efficiency is dependent on electrode geometries. The system chosen for simulation is copper sulfate solution of 0.1 (M) concentration with little supporting electrolyte. It is also noticed that migration effect remains important for supporting electrolyte concentration as high as 0.1 (M). Limiting current condition was assumed. © 2012 American Institute of Chemical Engineers *AIChE J,* 59: 1390–1399, 2013
Keywords: rotating ring disk electrode, ionic migration, presence of migration, absence of migration, collection efficiency

Introduction

The rotating ring disk electrode (RRDE) system is one of the most convenient arrangements of two working electrodes in a common cell. The concentric, rotating electrode structure is relatively easy to fabricate and is available commercially. The device has drawn attention and experimental applications. It has become a popular tool for the study of electrochemical reactions mainly because the hydrodynamics of the system are very well established and the transport equations can be solved very accurately. The RRDE has a unique feature that it can detect solution phase intermediates generated *in situ* in electrochemical reactions. Bruckenstein and Miller (1970)[1] have performed experiments with ring disks to assess the nonuniform current distribution on a disk electrode utilizing the sectioned electrode approach. Miksis and Newman (1976)[2] reported that the system of RRDE has three independent resistance values describing the primary potential difference between any two electrodes when current is passed between any two electrodes. Hessami and Tobias (1993)[3] reported experimental and theoretical analysis for *in situ* measurement of interfacial pH using a RRDE. Adanuvor et al. (1987)[4] modeled the rotating disk electrode (RDE) for studying kinetics of electrochemical reactions. Yen and Chapman (1987)[5] worked on migration effects with chemical reactions in electrochemical systems using RDE. They used orthogonal collocation technique to solve the transport-kinetic equations for determining the current distribution. Parikh and Liddell (1987)[6] also used orthogonal collocation technique to solve transport-kinetic equations for a RRDE system where excess of supporting electrolyte was considered so that effects of migration of ionic species in solution can be neglected.

The ring disk geometry contains two working electrodes (Figures 1 and 2) and a counter electrode can be utilized which would be considered infinitely far from the working electrodes. The working electrodes interact through potential distribution, current can flow between any of the three electrodes in the cell, but common experimental objectives usually attempt to limit the possibilities. The ring and the disk can be operated potentiostatically with the current from each electrode being collected by the counter electrode. The disk can be used to produce a species, not in the bulk solution, which can then be collected by the ring electrode, usually one electrode being driven cathodically and the other, anodically. Thus, the RRDE can be used to detect unstable solution phase intermediates generated *in situ* in electrochemical reactions.

Most of the past theoretical work with the RRDE has been restricted to situations where supporting electrolyte concentration is large enough so that the effect of migration of ionic species in the solution becomes negligible. The transport of species occurs by three transport mechanisms, namely, diffusion, convection, and migration. In presence of an excess of supporting electrolyte, the solution conductivity becomes appreciably high so that ohmic potential drop

Correspondence concerning this article should be addressed to S. Guha at sguha1968@yahoo.com.

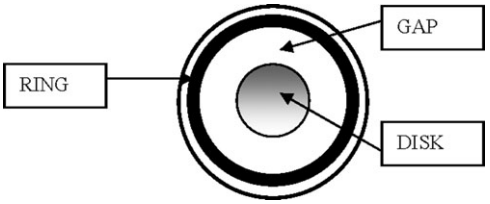

Figure 1. Schematic diagram of a RRDE.

becomes negligible. As result, the contribution of ionic migration to total transport becomes insignificant.

However, there are many situations, where the supporting electrolyte can not be used or its concentration is very low. In those cases neglect of migration will certainly incorporate large inaccuracy into the solution of transport equations. The situations where migration effect is of importance are anodic dissolution processes, metal deposition from binary salt solutions, metal deposition from a solution partially supported by acid etc.

Mathematical Modeling

Theory

There are three independent factors on which the current at an electrode depends. These are (a) transport of electro active species to and from electrode; (b) electron transfer at the electrode surface; and (c) kinetics of homogeneous reactions in the bulk electrolyte.

The transport of electro active species to the electrode surface occurs by three transport mechanisms namely ''Diffusion'' under a concentration gradient, which occurs within the concentration boundary layer, convection either natural or forced, owing to velocity of fluid and ''Migration'' due to presence of electric field.

If the electrode is operated under limiting current condition, then the concentration of the electro-active species, which is being transported to the electrode surface, becomes zero at the electrode surface and the current obtained at the electrode is the limiting current.

As pointed out earlier, the hydrodynamics of RRDE is very well-defined. The solution of equations of motion given by Cochran[7] (1934) for a disk rotating in solution (RDE) can be given for the radial and normal velocities as

$$v_r = Krx \tag{1}$$

$$v_x = -Kx^2 \tag{2}$$

Where constant K is given by

$$K = 0.510232\ w^{3/2}v^{-1/2} \tag{3}$$

The axial and radial velocities v_x and v_r, respectively are the same for RDE and RRDE.

It should be mentioned here that Eqs. 1 and 2 are valid for the case of infinite Schmidt number (Sc). Physically, this implies that the concentration boundary layer is much thinner than the hydrodynamic one. This is the case for most electrochemical systems of interest.

Assumptions

Following assumptions have been made while developing the mathematical model of the RRDE system:

1. The electrolyte is an ideal solution and, therefore, concentrations can be used in place of activities.
2. The disk surface is uniformly accessible.
3. Steady-state condition exists.
4. Isothermal condition exists.
5. The electrolyte is Newtonian and the physical and transport properties are constant.
6. Diffusivities of all reactants are constant.
7. Limiting current condition exists.
8. No homogeneous chemical reactions in bulk electrolyte.

Development of mathematical model

Fundamental Equations. The flux of a solute species is due to migration in an electric field, diffusion in a concentration gradient and convection with fluid velocity. The governing equation is:

$$N_i = -Z_iU_iFC_i\nabla\Phi - D_i\nabla C_i + vC_i \tag{4}$$

A material balance for a small volume element leads to differential conservation law:

$$\partial C_i/\partial t = -\nabla.N_i + R_i \tag{5}$$

As the reactions are restricted to the surface of electrodes in RRDE system, the bulk reaction term R_i is zero in this system. To a very good approximation, the solution is electrically neutral except in the diffuse part of the double layer very close to an interface, thus

$$\Sigma_iZ_iC_i = 0 \tag{6}$$

and

$$\partial C_i/\partial t = -\nabla.N_i \tag{7}$$

The current density in an electrolytic solution is due to the motion of charged species. The current density can be expressed as

$$I = F\Sigma_iZ_iN_i \tag{8}$$

These laws provide the basis for the analysis of electrochemical systems. The flux relation, Eq. 4 defines transport coefficients namely, the mobility U_i and the diffusion coefficient D_i of an ion in a dilute solution. The dilute solution theory is assumed.

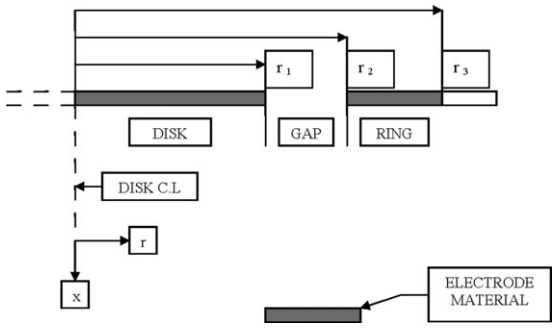

Figure 2. RRDE showing electrode geometries.

The RRDE system involves flow of the electrolytic solution. For an incompressible fluid of constant viscosity, the fluid velocity can be determined from the Navier-Stokes equation

$$\rho(\partial v/\partial t + v.\nabla v) = -\nabla P + \mu\nabla^2 v + \rho g \tag{9}$$

and the continuity equation

$$\nabla.v = 0 \tag{10}$$

Using the above fundamental equations for transport in dilute solutions, the general equation for the transport of species to the electrode surface for a RRDE system is developed which can be given in cylindrical co-ordinates as

$$\partial c/\partial t = D[(\partial^2 c/\partial x^2) + (\partial^2 c/\partial r^2) + 1/r(\partial c/\partial r)] - v_x(\partial c/\partial x) - v_r(\partial c/\partial r) + \mathrm{ZUF}[c(\partial^2\Phi/\partial x^2) + (\partial\Phi/\partial x)(\partial c/\partial x)], \tag{11}$$

where migration of the electroactive species has been taken into account. For the RRDE, however, radial diffusion is negligible compared to convective transport in the radial direction. Migration in radial direction can also be neglected. The diffusion coefficient (D) of species transporting is assumed to be constant through the diffusion layer and also mobility (U) is assumed constant in solution. Eq. 11 is now simplified to

$$\partial c/\partial t = D(\partial^2 c/\partial x^2) - v_x(\partial c/\partial x) - v_r(\partial c/\partial r) + \mathrm{ZUF}[c(\partial^2\Phi/\partial x^2) + (\partial\Phi/\partial x)(\partial c/\partial x)] \tag{12}$$

At steady-state condition $\partial c/\partial t = 0$, hence, Eq. 12 reduces to

$$D(\partial^2 c/\partial x^2) - v_x(\partial c/\partial x) - v_r(\partial c/\partial r) + \mathrm{ZUF}[c(\partial^2\Phi/\partial x^2) + (\partial\Phi/\partial x)(\partial c/\partial x)] = 0 \tag{13}$$

Governing Equations for Disk, Gap, and Ring Regions in Nondimensional Forms. With the help of aforementioned equations in hand, nondimensional governing equations have been developed for computer simulation of a RRDE system pertaining to a physical situation where an electron is transferred at the disk and the ring. This is done to ascertain effect of ionic migration on concentration variations of ionic species in normal and radial directions and the collection efficiencies of RRDE systems at various electrode geometries (β_1, β_2).

The system chosen for simulation is a binary salt solution of copper sulfate ($CuSO_4$) of 0.1 (M) concentration with very little supporting electrolyte which is sulfuric acid (H_2SO_4). Supporting electrolyte H^+ ion concentration in solution is considered as 0.02 (M). Supporting electrolyte H^+ ion concentration less than 0.02 (M) does not alter the results appreciably and hence not reported. It may be worth reporting here that setting the supporting electrolyte H^+ ion concentration equal to 0.0 (M) leads to divergence while solving the coupled ordinary and partial differential equations (ODEs and PDEs) for the disk, gap, and ring regions. This is purely due to problems associated with the numeric values while solving the coupled ODEs and PDEs numerically having the H^+ ion concentration exactly set equal to 0.0 (M). However, this problem of convergence has been circumvented by using very small non-zero values of supporting electrolyte H^+ ion concentration and it has been found that H^+ ion concentration value lower than 0.02 (M) does not alter the results appreciably and hence, the minimum supporting electrolyte concentration of 0.02 (M) has been reported. Eventually, if dimensionless potential profiles (Figure 3) are made, say for H^+ ion concentration values lower than 0.02 (M), all the curves more or less get superimposed on each other. Thus a single potential profile (Figure 3) corresponding to Supporting electrolyte H^+ ion concentration equal to 0.02 (M)(which represents presence of migration case) has been reported.

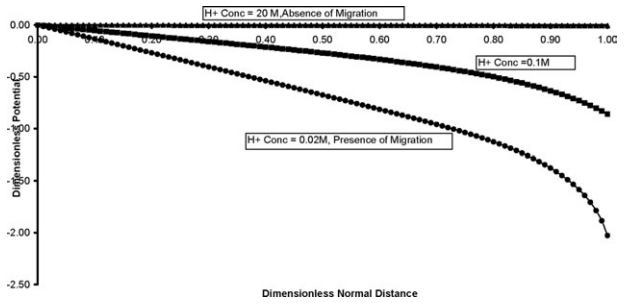

Figure 3. Dimensionless potential profiles at the disk.

The physical situation considered for simulation is enumerated below

$$Cu^{+2}(A) + e \rightarrow Cu^{+1}(B) \text{ at the disk}$$

$$Cu^{+1}(B) \rightarrow Cu^{+2}(A) + e \text{ at the ring}$$

$$SO_4^{-2}(C) \text{ is the conjugate ion}$$

Nondimensional Parameters The nondimensional variables with which the analysis has been made are defined below:

$$C_A^* = (C_{Ab} - C_A)/C_{Ab}, C_B^* = (C_{Ab} - C_B)/C_{Ab}, C_C^* = (C_{cb} - C_c)/C_{cb}$$

$$X = (K/D_A)^{1/3}x, R_1 = (r - r_1)/(r_2 - r_1), R_2 = (r - r_2)/(r_3 - r_2)$$

$$\Phi^* = (nF/RT)\Phi, \beta_1 = r_2/r_1, \beta_2 = r_3/r_2$$

where r_1,r_2, and r_3 define the geometry of the RRDE (Figure 2).

Nondimensional Equations for the Disk Region. The disk surface is generally assumed to be uniformly accessible because for a rotating disk, the hydrodynamics is such that the normal component of the velocity (Eq. 2) depends only on x, the normal distance from the disk. Consequently, concentration and potential also depends only on x in the diffusion layer, the limiting current density is uniform over the surface of the disk. Thus, the assumption of uniform current distribution enables us to drop the gradient in the radial direction for the disk region.

Thus the equation for transport of A to the disk surface in nondimensional form using dimensionless variables defined above is as given below

$$d^2C_A^*/dX^2 + X^2(dC_A^*/dX) - (Z_A U_A RT/nD_A)[(1 - C_A^*)(d^2\Phi^*/dX^2) - (dC_A^*/dX)(d\Phi^*/dX)] = 0 \tag{14}$$

and similarly for the conjugate ion (C), the equation of transport is

$$d^2C_C^*/dX^2 + X^2(dC_C^*/dX) - (Z_cU_cRT/nD_c)$$
$$[(1 - C_C^*)(d^2\Phi^*/dX^2) - (dC_C^*/dX)(d\Phi^*/dX)] = 0 \quad (15)$$

The electro neutrality condition is given by

$$Z_AC_{Ab}(1 - C_A^*) + Z_cC_{cb}(1 - C_C^*) = 0 \quad (15a)$$

With the boundary conditions:

$$X = 0, C_A^* = 1, \Phi^* = (nF/RT)\Phi_o, dC_C^*/dX = 0$$
$$X = 1, C_A^* = 0, C_C^* = 0, \Phi^* = (nF/RT)\Phi_{re}$$

$X = 1$ corresponds to $x = x_{max} = {}_{(K/D_A)}{}^{-1/3}$. x_{max} being the normal distance from the disk surface where concentration of A reaches the bulk concentration.

It should be noted here that the electrode reaction, $Cu^{+2}(A) + e \rightarrow Cu^{+1}$ (B) occurs at the disk and the unstable solution phase intermediate species, $Cu^{+1}(B)$ is generated *in situ* at the disk and is eventually collected by the ring electrode where the electrode reaction $Cu^{+1}(B) \rightarrow Cu^{+2}$ (A) + e takes place. The ring electrode collects part of the total material generated at the disk ($Cu^{+1}(B)$) and the rest is lost into bulk electrolyte.

Nondimensional Equations for the Gap Region. The component B produced at the disk surface is transported across the insulating gap to the ring electrode by convection, diffusion, and migration. The equation for the transport of B across the gap may be given in nondimensional form as

$$(\partial^2C_B^*/\partial X^2) - X[R_1 + 1/(\beta_1 - 1)](\partial C_B^*/\partial R_1) + X^2(\partial C_B^*/\partial X)$$
$$- (Z_BU_BRT/nD_B)[(1 - C_B^*)(d^2\Phi^*/dX^2)$$
$$-(d\Phi^*/dX)(\partial C_B^*/\partial X)] = 0 \quad (16)$$

Where $\beta_1 = r_2/r_1$ (gap thickness)

The equation for transport of C which is the conjugate ion is given by:

$$(\partial^2C_C^*/\partial X^2) - X[R_1 + 1/(\beta_1 - 1)](\partial C_C^*/\partial R_1) + X^2(\partial C_C^*/\partial X)$$
$$- (Z_cU_cRT/nD_c)[(1 - C_C^*)(d^2\Phi^*/dX^2)$$
$$-(d\Phi^*/dX)(\partial C_C^*/\partial X)] = 0 \quad (17)$$

The electroneutrality condition is given by

$$Z_AC_{Ab}C_B^* + Z_cC_{cb}(1 - C_C^*) = 0 \quad (18)$$

Now if the diffusivities of A and B are equal and a simple electron transfer occurs at the disk and at the ring then it can be shown by a material balance that

$$C_B^* = 1 - C_A^* \quad (19)$$

In this case, the boundary condition may be written as

$$X = 0, \partial C_B^*/\partial X = 0, \Phi^* = 0, \partial C_C^*/\partial X = 0$$
$$X = 1, C_B^* = 1, C_C^* = 0, \Phi^* = (nF/RT)\Phi_{re}$$
$$R_1 = 0, C_B^* = 1 - C_A^*, C_C^* = C_A^*$$

The boundary condition at $X = 0$ merely indicates that there can be no flux of material at the surface in the insulating gap and also no applied potential. The boundary condition at $R_1 = 0$, indicates that the concentration at the outer edge of the disk is equal to the concentration at the inner edge of the gap, thus maintaining continuity between two regions.

Nondimensional Equations for the Ring Region. The equation for mass transport in the ring region in nondimensional form may be expressed as

$$(\partial^2C_B^*/\partial X2) - X[R_2 + 1/(\beta_2 - 1)](\partial C_B^*/\partial R_2) + X^2(\partial C_B^*/\partial X)$$
$$- (Z_BU_BRT/nD_B)[(1 - C_B^*)(d^2\Phi^*/dX^2)$$
$$-(d\Phi^*/dX)(\partial C_B^*/\partial X)] = 0 \quad (20)$$

Where $\beta_2 = r_3/r_2$ (ring thickness)

The equation for transport of C which is the conjugate ion is given by

$$(\partial^2C_C^*/\partial X^2) - X[R_2 + 1/(\beta_2 - 1)](\partial C_C^*/\partial R_2) + X^2(\partial C_C^*/\partial X)$$
$$- (Z_cU_cRT/nD_c)[(1 - C_C^*)(d^2\Phi^*/dX^2)$$
$$-(d\Phi^*/dX)(\partial C_C^*/\partial X)] = 0 \quad (21)$$

And the electroneutrality relation is given as

$$Z_AC_{Ab}C_B^* + Z_cC_{cb}(1 - C_C^*) = 0 \quad (22)$$

The boundary conditions may be written as

$$X = 0, C_B^* = 1, \Phi^* = (nF/RT)\Phi_o, \partial C_C^*/\partial X = 0$$
$$X = 1, C_B^* = 1, C_C^* = 0, \Phi^* = (nF/RT)\Phi_{re}$$
$$R_2 = 0, C_B^* = C_B^*(gap), C_C^* = C_C^*(gap)$$

As mentioned earlier, the boundary condition at $R_2 = 0$ signifies that the concentration at the outer edge of the gap is equal to that at the inner edge of the ring.

Estimation of Collection Efficiency. Collection efficiency, N is the ratio of amount of material detected at the ring to the amount produced at the disk. As the concentration and current are directly related, this parameter gives the relationship between the ring current and the disk current, as

$$N = -I_R/I_D \quad (23)$$

The current at the disk I_D is calculated as

$$I_D = -nFA_sD_A[dC_A/dx]_{x=0} \quad (24)$$

This is directly proportional to the concentration gradient in normal direction at the disk surface. The ring current is directly proportional to the gradient of concentration of component B in the normal direction. The concentration of B is nonuniform across the ring surface unlike that for the disk. The gradient, thus, has to be integrated over the ring surface to obtain the ring current, this is expressed as

$$I_R = 2nFD_B\Pi\int_{r_2}^{r_3}[\partial C_B/\partial x]_{x=0}\, rdr \quad (25)$$

Substituting for I_D and I_R from Eqs. 24 and 25 and assuming $D_A = D_B$ (for all practical purposes) into Eq. 23 we have

$$N = 2/[dC_A/dx]_{x=0} r_1^2 \int_{r_2}^{r_3} [\partial C_B/\partial x]_{x=0}\, r dr \qquad (26)$$

Introducing nondimensional parameters defined earlier, we have

$$N = 2/[dC_A^*/dx]_{x=0} r_1^2 \int_0^1 [\partial C_B^*/\partial x]_{x=0}[(r_3 - r_2)R_2 + r_2](r_3 - r_2)dR_2 \qquad (27)$$

Or

$$N = 2/[dC_A^*/dx]_{x=0} \int_0^1 [((\beta_1\beta_2)^2 + \beta_1^2 - 2\beta_1^2\beta_2)R_2 + \beta_1^2\beta_2 - \beta_1^2]dR_2 \qquad (28)$$

Results and Discussion

The dimensionless equations for the disk, gap, and ring regions were solved on a high-speed computer using explicit finite difference numerical technique. Due to stability constraint of explicit finite difference numerical technique, the optimum step sizes chosen in normal (x) and radial (r) directions are 0.046 and 0.005, respectively. The step sizes in normal (x) and radial (r) directions have been optimized based on the general convergence criteria $D\Delta t/(\Delta x)^2 \leq 0.5$ for a parabolic partial differential equation of the form

$$\partial c/\partial t = D(\partial^2 c/\partial x^2). \qquad (29)$$

In this work, term like $D\Delta R/(\Delta X)^2$ has been used for optimizing the step sizes in normal (x) and radial (r) directions.

Two cases were compared, namely "in presence of migration" and "in absence of migration" to ascertain the effect of ionic migration on concentration variations of ionic species in normal and radial directions and collection efficiencies at varying electrode geometries.

The physical situation, as described earlier, has been chosen where an electron is transferred at the disk and the ring

$$Cu^{+2}(A) + e \rightarrow Cu^{+1}\ (B) \text{at the disk}$$

$$Cu^{+1}(B) \rightarrow Cu^{+2}(A) + e \text{ at the ring}$$

$$SO_4^{-2}(C) \text{ is the conjugate ion}$$

The system considered is a binary salt solution of copper sulfate ($CuSO_4$) of 0.1 (M) concentration with very little supporting electrolytes (H^+ ion concentration = 0.02 (M)) for presence of migration case. Conversely, for the case of absence of migration, copper sulfate ($CuSO_4$) of 0.1 (M) concentration along with Sulfuric acid (H_2SO_4) concentration of 10 (M) (H^+ ion concentration = 20 (M)) was considered as supporting electrolyte. Supporting electrolyte concentration of more than 10 (M) was not considered as potential variation loses its practical significance beyond this concentration (Figure 3). Moreover, supporting electrolyte H^+ ion concentration less than 0.02 (M) does not alter the results appreciably and hence not reported. Ring and disk has been assumed to operate potentiostatically. Fixed disk radius considered is 0.4 cm and speed of rotation considered is 900 rpm. System temperature is considered as 25°C. Limiting current condition has been assumed.

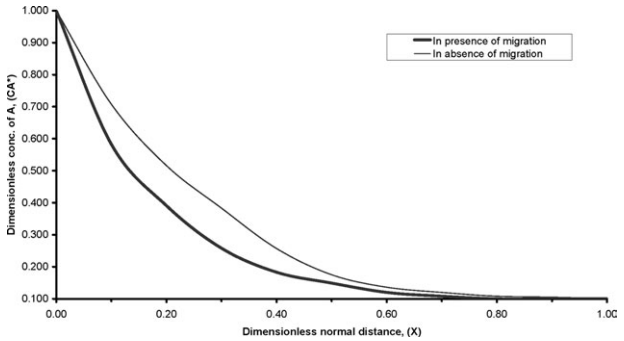

Figure 4. Dimensionless concentration profiles at the disk.

Discussion on importance of migration with respect to supporting electrolyte concentration

In Figure 3, dimensionless potential (Φ^*) has been plotted against dimensionless normal distance (X) for three cases namely, supporting electrolyte H^+ concentration of 0.02 (M), supporting electrolyte H^+ concentration of 0.1 (M), and supporting electrolyte H^+ concentration of 20 (M).

As can be seen from the curves that when there is no or very little supporting electrolyte in the solution (H^+ concentration of 0.02 (M)), the dimensionless potential gradient is very high in the solution which indicates that migration mode of transport is of considerable importance.

Alternatively, in case of supporting electrolyte concentration is moderately high (H^+ concentration of 0.1 (M)), the dimensionless gradient of potential falls to a large extent due to enhancement of solution conductivity and it is observed that beyond this supporting electrolyte concentration, dimensionless potential variation loses its practical significance and hence not considered. Eventually, the plot of Φ^* versus X for supporting electrolyte H^+ concentration of 20 (M) results into a horizontal line.

Discussion on effects of migration for Disk of RRDE

In Figure 4 dimensionless concentration of reactant A (C_A^*) is plotted against the dimensionless normal distance from the disk surface (X) for two cases; (1) in presence of migration of ions, and (2) in absence of migration of ions. The plot of the second case is well known Levich[8] (1962) solution. Levich had analyzed the mass transfer to a RDE[11] where convective-diffusion was considered as transport mechanism for ionic species (i.e., situation same as "absence of migration" case). The governing equation for convective-diffusion was given as

$$v_x(dC_i/dx) = D_i(d^2C_i/dx^2) \qquad (30)$$

with boundary conditions as (i) $C_i = 0$ at $x = 0$ (i.e., at the disk surface) at the limiting current condition and (ii) $C_i = C_{ib}$ at $x = \infty$ (i.e., at the bulk electrolyte).

The solution to the above equation (Eq. 30) was given for limiting current condition, as

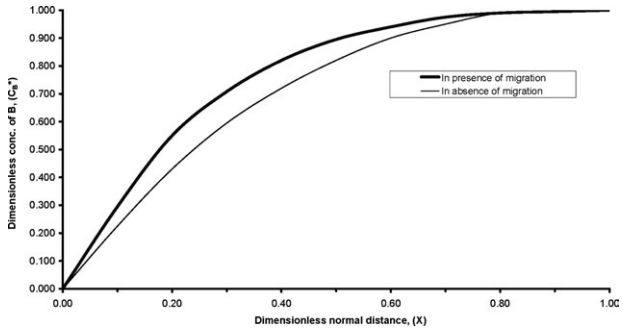

Figure 5. Dimensionless concentration variation in normal direction at the gap.

Dimensionless radial distance, R_1= 0 (inner edge of the gap) dimensionless gap and ring thicknesses = 1.02.

$$C_i/C_{ib} = \left[\int_0^x \exp\left(\int_0^x (v_x/D_i)dx\right)dx\right] \Big/ \left[\int_0^\infty \exp\left(\int_0^x (v_x/D_i)dx\right)dx\right] \quad (31)$$

The plot of the second case, (i.e., ''absence of migration'') is analogous to Levich solution in nondimensional form where migration terms have been neglected with boundary conditions ''as described under section entitled Nondimensional equations for the disk region'' neglecting the boundary conditions pertaining to Φ*.

From the curves, it can be seen that in the case where migration of ions is present, the concentration boundary layer thickness has reduced. The reduction is about 30% of the thickness of the concentration boundary layer, existing when migration of ions is absent. This is due to the fact that in presence of migration, the molar flux of ionic species towards the disk electrode is higher than compared with the flux present while migration is absent. The result is that the variation of concentration is limited to shorter distance from the disk surface, thereby decreasing the thickness of the concentration boundary layer. Due to enhancement of molar flux of ionic species towards the disk, the limiting current at the disk increases. Eventually, the limiting current at the disk will get reduced if supporting electrolyte is added to the system. The reason being the supporting electrolyte will increase solution conductivity and hence, the migration mode of transport will become insignificant. This will result in smaller molar flux of ionic species towards the disk.

As can be seen, the curve for the case where migration mode of transport is absent lies above the curve for the case when migration is present. This is because of the fact that since concentration boundary layer thickness decreases in presence of migration, concentration of reactant A (Cu^{+2}) is higher at any normal position in the boundary layer compared to the concentration at the same position when migration is absent.

Discussion on effects of migration for gap of RRDE

Concentration Variation in Normal Direction. In Figure 5, dimensionless concentration of B (C_B^*) is plotted against the dimensionless normal distance from the disk surface (X) for both the cases namely presence and absence of migration. The profiles are for the dimensionless radial distance $R_1 = 0$, that is, at the inner edge of the gap or at the outer edge of the disk. The shapes of the curves in Figure 5 are similar to that in Figure 4 except that instead of dimensionless concentration of A, (C_A^*), dimensionless concentration of B, (C_B^*) is plotted which is obtained from the simple material balance, $C_B^* = 1-C_A^*$. Thus at $X = 0$, $C_A^* = 1.0$ and hence, $C_B^* = 0$, whereas at $X = 1$, $C_B^* = 1$ and hence, $C_A^* = 0$.

Moreover, as the boundary condition at the gap surface is such that the flux of material B at the surface of the gap is zero, that is, $\partial C_B^*/\partial X = 0$ at $X = 0$, which also implies that $C_B^* = 0$ at the surface of the gap, the curve start from (0, 0). The plot satisfies the boundary condition, $C_B^* = 1-C_A^*$ at $R_1 = 0$, that is, at the inner edge of the gap or at the outer edge of the disk, thus maintaining continuity between two regions.

As can be seen, the curve for the case where migration is present lies above the curve where migration is absent. This is due to the fact that in presence of migration, the flux of material B toward the bulk becomes high due to the additional transport by migration compared to that in case of absence of migration and hence, the concentration gradient of B in normal direction becomes higher at all normal positions compared to that in absence of migration.

Figure 6 shows variation of C_B^* with X at R_1=1.0, that is, at the outer edge of the gap or at the inner edge of the ring, for both the cases, in presence and in absence of migration. As can be seen from the curves, the dimensionless concentrations are very high both the cases, which implies that the concentration of product B is relatively small at the outer edge of the gap. This is due to loss of material B into the bulk during its transport in radial direction.

The reason for the fact that the curve in case of presence of migration lies above the curve in case of absence of migration is as given below:

In presence of migration, the concentration gradient of component B in normal direction is higher due to presence of an additional mode of transport of ionic species towards the bulk and as a result of which the molar flux of species B is higher towards the bulk leading to lesser concentration throughout the concentration boundary layer.

Concentration Variation in Radial Direction. Figure 7 shows dimensionless concentration variation in radial direction at dimensionless normal distance $X = 0.01$, that is, close to the surface of the gap of RRDE for both the cases, namely in presence and in absence of migration.

It is seen that the concentration of component B is smaller at all radial positions in presence of migration than that in absence of migration. The reason for the above fact is that in case of presence of migration, normal flux of component

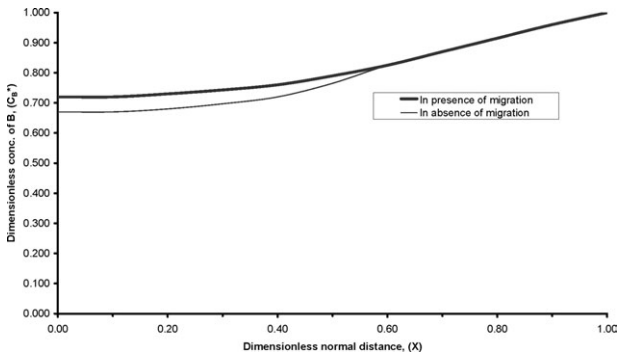

Figure 6. Dimensionless concentration variation in normal direction at the gap.

Dimensionless radial distance, R_1 = 1(outer edge of the gap) dimensionless gap and ring thicknesses = 1.02.

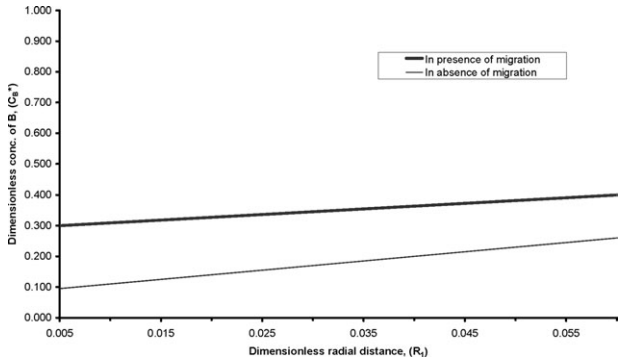

Figure 7. Dimensionless concentration variation in radial direction at the gap.

Dimensionless normal distance, $X = 0.01$ (close to the gap surface) dimensionless gap and ring thicknesses = 1.02.

B is higher due to higher normal concentration gradient and as a result of which the concentration of B falls all along the radial direction.

It may also be pointed out here that the curve representing absence of migration case has somewhat higher slope at the beginning than that for the curve where migration is present. This is due to the fact that in presence of migration, concentration gradient falls in the radial direction and as a result, the slope for the case where migration is absent is slightly higher than that for the case where migration is present.

Figures 8–10 provide the dimensionless concentration variation in radial direction at dimensionless normal distances $X = 0.2$, 0.4, and 0.8, respectively for both the cases, in presence and in absence of migration of ionic species.

As can be seen from Figure 8, both the profiles are almost flat straight lines. Strictly speaking, they should show a small positive slope in the radial direction. The reason for the fact that the curves are almost flat instead of having positive slope comes from the fact that in normal direction, the concentration of B falls very rapidly and hence, in the simulation, it has been found that values of concentration of B changes after fourth decimal place and therefore, for all practical purposes, the variation can be neglected. Thus we observe these flat profiles.

The results in Figure 9 and 10 are similar to those in Figure 8 except that the concentration of B decreases with increase in X for both the cases, namely presence and absence of migration which is as would be expected.

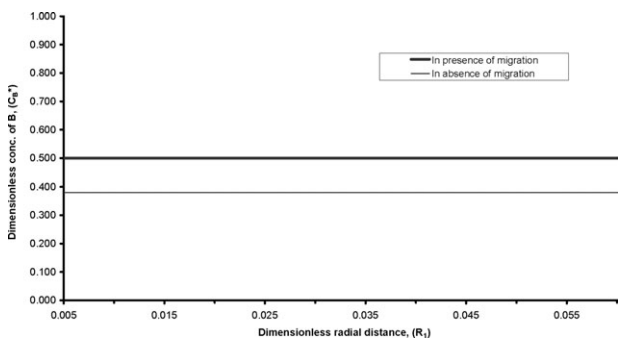

Figure 8. Dimensionless concentration variation in radial direction at the gap.

Dimensionless normal distance, $X = 0.2$ dimensionless gap and ring thicknesses = 1.02.

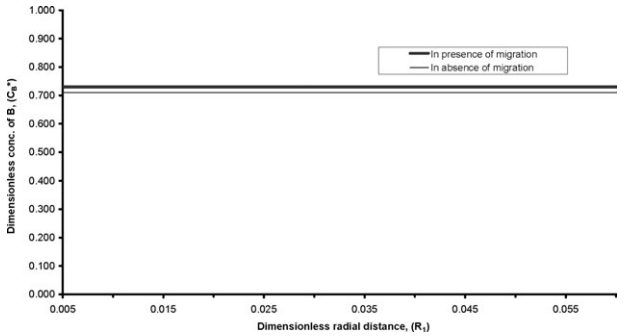

Figure 9. Dimensionless concentration variation in radial direction at the gap.

Dimensionless normal distance, $X = 0.4$ dimensionless gap and ring thicknesses = 1.02.

Discussion on effects of migration for Ring of RRDE

Concentration Variation in Normal Direction. In Figure 11, dimensionless concentration variations are shown in normal direction at the dimensionless radial distance $R_2 = 0.01$(inner edge of the ring) for both the cases, in presence and in absence of migration. The profiles show minima at a dimensionless normal distance of 0.1. This implies that the concentration of B goes through maxima in the normal direction for both the cases. The reason for this comes from the fact that at the surface of the ring, B gets converted to A by the electrode reaction: $B \rightarrow A + ne$ and hence, at the surface, the concentration of B falls to zero. The concentration of B is also zero at the bulk. Hence, in the diffusion layer, concentration of B passes through maxima for both the cases.

It can also be seen, the minimum dimensionless concentration of B is lower in case of presence of migration as compared to that in case of absence of migration. This implies that maximum concentration of B is higher in presence of migration than that in absence of migration. The reason for this fact is that in case of presence of migration, the boundary layer thickness reduces and as a result of which the concentration of product B increases within the boundary layer and since concentration of B at the ring electrode surface is zero, the normal gradient is high in case of presence of migration which leads to higher mass flux towards the ring. Thus the collection efficiency is expected to increase in presence of migration.

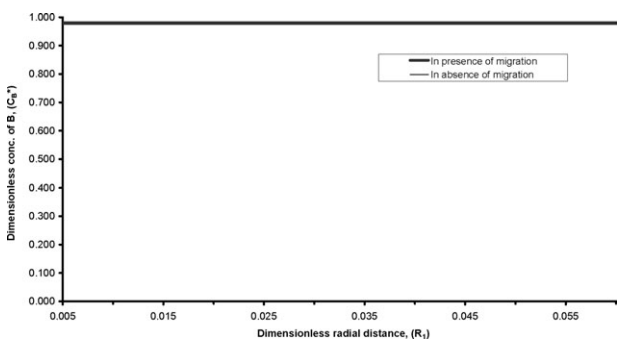

Figure 10. Dimensionless concentration variation in radial direction at the gap.

Dimensionless normal distance, $X = 0.8$ dimensionless gap and ring thicknesses = 1.02.

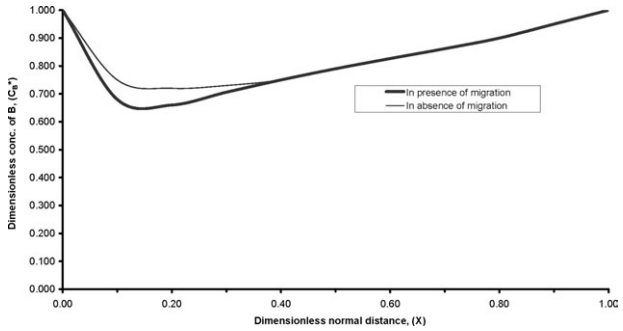

Figure 11. Dimensionless concentration variation in normal direction at the ring.

Dimensionless radial distance, $R_2 = 0.01$ (inner edge of the ring) dimensionless gap and ring thicknesses = 1.02.

Concentration Variation in Radial Direction. Figures 12–15 show the dimensionless concentration variation of B in radial direction (R_2) at the dimensionless normal distances, $X = 0.01$, $X = 0.2$, $X = 0.4$, and $X = 0.8$, respectively for both the cases, in presence and in absence of migration.

The figures indicate that concentration of component B is lower at all radial positions in presence of migration compared to that in absence of migration. This is due to the fact that as described earlier, the molar flux of material B toward the ring electrode is higher due to higher normal concentration gradient compared to that in absence of migration. Thus, concentration at any normal position in the radial direction is lower in presence of migration than in absence of migration.

It is also seen that the concentration levels are decreasing with increasing X which merely indicates that material B is also getting transported toward the bulk region. It may also be pointed out here that the difference in concentration for the two curves nearly vanishes close to boundary layer. This is because, close to the boundary layer, the concentration of B is so low for both the cases that there is hardly any difference between them.

Discussion on effects of migration on Collection Efficiency in a RRDE

In Table 1, a comparison between collection efficiencies[9] in presence and in absence of migration for different electrode geometries is presented.

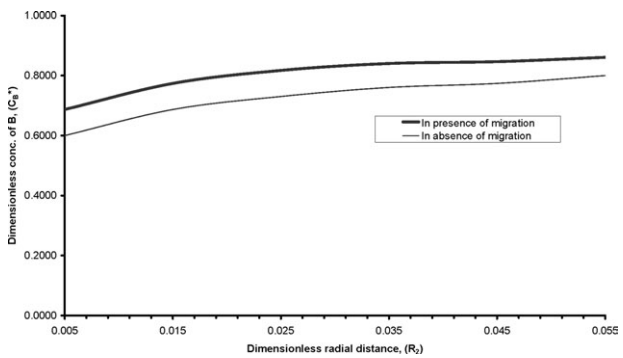

Figure 12. Dimensionless concentration variation in radial direction at the ring.

Dimensionless normal distance, $X = 0.01$ dimensionless gap and ring thicknesses = 1.02.

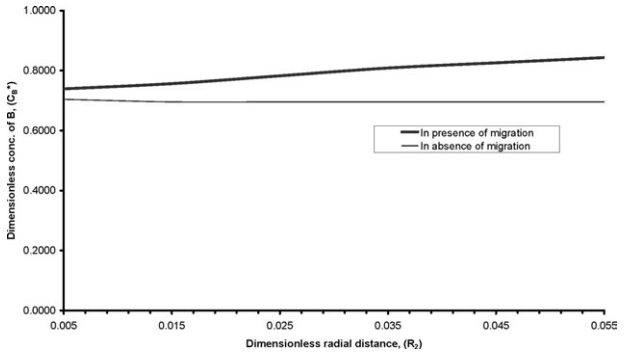

Figure 13. Dimensionless concentration variation in radial direction at the ring.

Dimensionless normal distance, $X = 0.2$ dimensionless gap and ring thicknesses = 1.02.

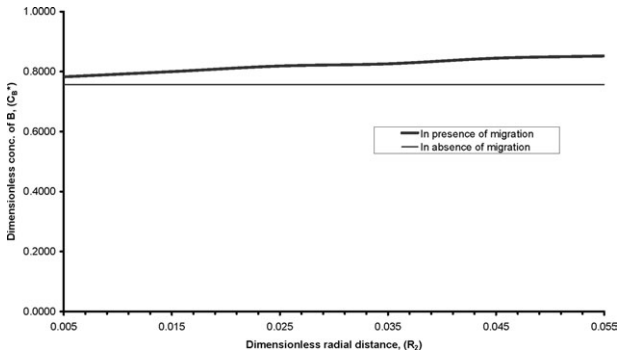

Figure 14. Dimensionless concentration variation in radial direction at the ring.

Dimensionless normal distance, $X = 0.4$ dimensionless gap and ring thicknesses = 1.02.

As can be seen from Table 1, the collection efficiency is higher in case of presence of ionic migration than the case where migration of ions is absent for all electrode geometries.

The above is due to the fact that in presence of migration, total amount of mass transport to the ring surface is higher because of one additional mode of transport (migration), and hence, larger amount of material is collected at the ring, less is lost to the bulk leading to increase in collection efficiency.

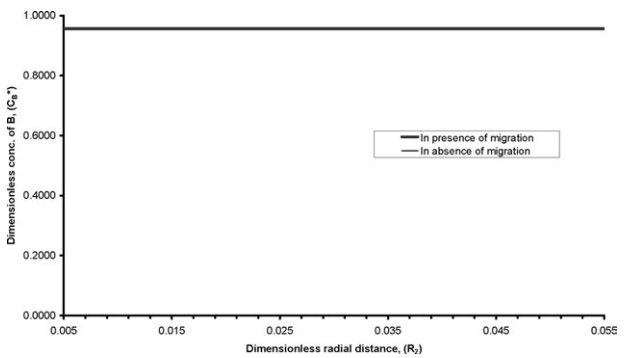

Figure 15. Dimensionless concentration variation in radial direction at the ring.

Dimensionless normal distance, $X = 0.8$ dimensionless gap and ring thicknesses = 1.02.

Table 1. Comparison Between Collection Efficiencies in Presence and in Absence of Migration for Different Electrode Geometries

RRDE Geometrical Parameters		Collection Efficiency (N)	
$\beta_1 = r_2/r_1$	$\beta_2 = r_3/r_2$	In presence of migration	In absence of migration
1.02	1.02	0.201647	0.10279
1.04	1.02	0.1874241	0.09569
1.02	1.005	0.042019	0.04200
1.09	1.02	0.1443830	0.08569
1.10	1.02	0.1403571	0.08431
1.02	1.015	0.1716025	0.08618
1.06	1.02	0.1628195	0.09087
1.02	1.01	0.1356836	0.06690

Also, as mentioned earlier, in presence of migration, flux of material B (Cu^{+1}) is higher at the ring surface than in absence of migration. This is in accordance with the higher collection efficiency in presence of migration than in its absence.

As it is well-known that the collection efficiency is function of geometrical parameters of a RRDE, such as gap thickness (β_1) and ring thickness (β_2), the variation of collection efficiency with these parameters has been investigated for the case where migration is present and also for the case where it is absent. In Figure 16, collection efficiency, N has been plotted against the ring thickness (β_2) for constant gap thickness (β_1) as 1.02. The disk radius is taken as 0.4 cm. The plots are made for both the cases, in presence and in absence of migration.

As can be seen from Figure 16, in both the cases, in presence and in absence of migration, the collection efficiency rises with increase in ring thickness. This is because as the ring thickness increases, surface area of electrode reaction becomes high at the ring and hence, larger amount of material is collected by the ring leading to enhancement of collection efficiency.

In case of presence of migration, due to presence of an additional mode of transport, the rate of increase in collection efficiency is higher than that for the case where migration is absent and hence the bold solid curve lies above the thin solid one.

In Figure 17, collection efficiency, N is plotted against the gap thickness (β_1) for constant ring thickness (β_2) as 1.02, for both the cases, in presence and in absence of migration.

It can be seen from the plots, the collection efficiency falls with increasing gap thickness (β_1) for both the cases. This is due to the fact that larger the thickness of the gap, more of the species generated at the disk is carried over to the bulk solution rather than to the ring surface and therefore, lesser quantity of material is detected at the ring leading to a reduction in collection efficiency.

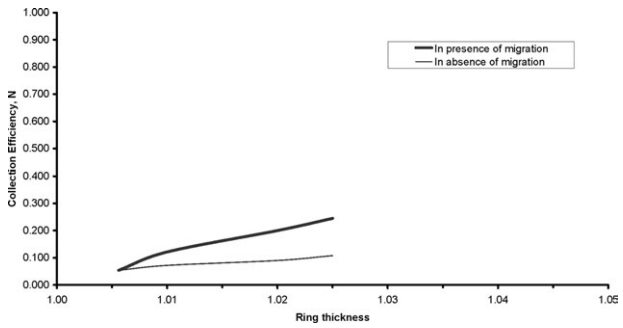

Figure 16. Collection efficiency variation with ring thickness for constant gap thickness (gap thickness = 1.02; disk radius = 0.4 cm).

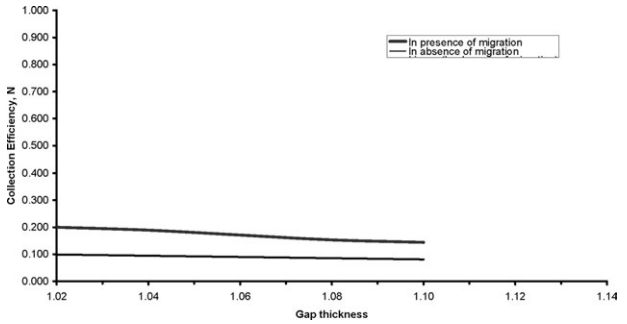

Figure 17. Collection efficiency variation with gap thickness for constant ring thickness (ring thickness = 1.02; disk radius = 0.4 cm).

Conclusions

Most of the past research work with the RRDE has been restricted to situations where migration of ionic species had been neglected because of presence of excess of supporting electrolyte in the solution.[10] Nevertheless, there are many situations where excess of supporting electrolyte is not present or the supporting electrolyte concentration is appreciably low. As for example, anodic dissolution process, metal deposition from binary salt solution, metal deposition from a solution partially supported by acid etc., are some of the many situations where supporting electrolyte concentration is very little or zero. In those situations, migration plays an important role for transport of species from the bulk solution to the electrode, and, hence, currents at the electrode changes. Thus, it can be inferred from the above discussion that neglect of migration in some electrochemical processes will incorporate appreciable error in the analysis.

Due to the above reasons, efforts have been made to investigate the effect of migration on certain important electrochemical parameters, such as concentration, current and collection efficiency using a RRDE system. It has been found that migration does have profound effect on potential and concentration distributions, limiting currents and collection efficiencies at all electrode geometries at disk, gap, and ring of a RRDE. It has also been determined that in presence of migration, the concentration boundary layer thickness reduces leading to higher rate of mass transport toward the RRDE. Due to reduction in concentration boundary layer thickness, the normal concentration gradient becomes high and as a result the collection efficiency increases.

Electrochemical parameters[12–20] are frequently determined by fitting data to theoretical curves similar to those presented here. This work clearly shows that neglect of migration in the theoretical analysis in systems involving appreciable migration can lead to considerable error in estimation of the parameters.

Notation

A_s = surface area or disk electrode, cm^2
A = cupric ion, Cu^{2+}
B = cuprous ion, Cu^{+}
C = sulfate ion, SO_4^{2-}
c = concentration, mole/cc

C_i = concentration of species i, mole/cc
C_A = concentration of species A, mole/cc
C_B = concentration of species B, mole/cc
C_C = concentration of species C, mole/cc
C_A^* = dimensionless concentration of species A
C_B^* = dimensionless concentration of species B
C_C^* = dimensionless concentration of species C
C_{Ab} = concentration of species A in the bulk, mole/cc
C_{Cb} = concentration of species C in the bulk, mole/cc
C_{ib} = concentration of species i in the bulk, mole/cc
D = diffusivity, cm^2/sec
D_A = diffusivity of species A, cm^2/sec
D_B = diffusivity of species B, cm^2/sec
D_C = diffusivity of species C, cm^2/sec
D_i = diffusivity of species i, cm^2/sec
F = Faraday's constant, 96487 C/equiv
g = acceleration due to gravity
I = current density, amp/cm^2
I_R = current at the ring, C/sec
I_D = current at the disk, C/sec
K = constant (defined in Eq. 3)
n = no. of electrons
N = collection efficiency
N_i = molar flux of species i, mole/cm^2 sec
r = radial distance, cm
R_1 = dimensionless radial distance at the gap region
R_2 = dimensionless radial distance at the ring region
R_i = reaction rate in bulk solution
r_1 = radius of disk, cm
r_2 = outer radius of the gap, cm
r_3 = outer radius of the ring, cm
R = universal gas constant, 8.3144 J/mol K
Sc = Schmidt number
t = time, sec
T = temperature, K
U = ionic mobility, cm^2-mole/J sec
U_i = ionic mobility of ith species, cm^2 mole/J sec
U_A = ionic mobility of species A, cm^2 mole/J sec
U_B = ionic mobility of species B, cm^2 mole/J sec
U_C = ionic mobility of species C, cm^2 mole/J sec
v = velocity, cm/sec
v_x = velocity in x–direction, cm/sec
v_r = velocity in r–direction, cm/sec
w = revolutions per sec, sec^{-1}
x = normal distance from electrode surface, cm
X = dimensionless normal distance from electrode surface
x_{max} = edge of the concentration boundary layer, cm
Z_i = charge number on species i
Z_A = charge number on species A
Z_B = charge number on species B
Z_C = charge number on species C
$\beta_1 = r_2/r_1$, gap thickness
$\beta_2 = r_3/r_2$, ring thickness
Φ = potential, volt
Φ^* = dimensionless potential
Φ_o = constant potential applied at the disk, volt
Φ_{re} = reference potential, volt
ρ = density of solution, gm/cc
P = pressure, dyne/cm^2
μ = viscosity, gm/cm.sec
v = kinematic viscosity, cm^2/sec

Literature Cited

1. Bruckenstein S, Miller B. An experimental study of non uniform current distribution at rotating disk electrodes. *J Electrochem Soc*. 1970;117:1044–1048.
2. Miksis JJ, Newman JS. Primary resistance for ring disk electrodes. *J Electrochem Soc*. 1976;123:1030–1036.
3. Hessami S, Tobias CW. In-situ measurement of interfacial PH using a rotating ring disk electrode. *AIChE J*. 1993;39:149–162.
4. Adanuvor PK, White RE, Lorimer SE. Modeling the rotating disk electrode for studying the kinetics of electrochemical reactions. *J Electrochem Soc*. 1987;134:625–631.
5. Yen SC, Chapman TW. Current distribution on a rotating disk electrode: effects of migration and reactions. *J Electrochem Soc*. 1987;134:1964–1972.
6. Parikh RS, Liddell KC. Ph. D. Thesis. Orthogonal collocation simulation of the RRDE. Washington State University; 1987.
7. Cochran WG. The flow due to a rotating disk. *Proc Camb Philos Soc*. 1934;30:365–375.
8. Levich VG. *Physicochemical Hydrodynamics*. Englewood, Cliffs NJ: Prentice Hall, 1962.
9. Albery WJ, Brukenstein S. Ring disc electrodes, Part 2. Theoretical and experimental collection efficiencies. *Trans Faraday Soc*. 1966;62:1920–1931.
10. Sirshendu G. Parikh RS. M.Tech. Thesis. Simulation of the RRDE incorporating ionic migration. Delhi: Indian Institute of Technology; 1994.
11. Forbes M, Lynn S. Oxygen reduction at an anodicauy activated platinum rotating disk electrode. *AIChE J*. 1975;21:763–769.
12. Newman JS. *Electrochemical Systems*. Englewood, Cliffs NJ: Prentice Hall Inc., 1962.
13. Mandin Ph, Fabian C, Lincot D. Numerical simulation of hydrodynamic and mass-transport properties at a laminar Rotating cylinder electrode. *J Electrochem Soc*. 2006;153(3):D40–D50.
14. Mandin Ph, Fabian C, Lincot D. Mean and unsteady hydrodynamic and mass transport properties at a rotating cylinder electrode: from laminar to transitional flow regime. *J Electroanal Chem*. 2006; 586(2):276–296.
15. Mandin Ph, Fabian C, Lincot D. Importance of the density gradient effects in modeling electro-deposition process at a rotating cylinder electrode. *Electrochim Acta*. 2006;51(19):4067–4079.
16. Mandin Ph, Ceuse JM, Picard G, Lincot D. Simplified kinetic modeling and numerical simulation of a metal oxide chemical bath electro-deposition process at a rotating electrode. *Electrochim Acta*. 2006;52(3):1296–1308.
17. Mandin Ph, Ceuse JM, Georges B, Favre V, Pauporte Th, Fukunaka Y, Lincot D. Prediction of the electro-deposition process behavior with the gravity or acceleration value at continuous and discrete scale. *Electrochim Acta*. 2007;53(1):233–244.
18. Mandin Ph, Pauporte Th, Fanouillere Ph, Lincot D. Modeling and numerical simulation of hydro-dynamical process in a confined rotating electrode configuration. *J Electroanal Chem*. 2004;565(2): 159–173.
19. Szanto DA, Cleghorn S, Ponce-de-Leon C, Walsh FC. The limiting current for reduction of ferricyanide ion at nickel: the importance of experimental conditions. *AIChE J*. 2008;54:802–810.
20. Yang JD, West AC. Current distributions governed by coupled concentration and potential fields. *AIChE J*. 1997;43:811–817.

Manuscript received Dec. 7, 2011, and revision received Mar. 31, 2012.